Acta Geod Geophys (2013) 48:149–161
DOI 10.1007/s40328-012-0010-4

Performance assessment of GPS/GLONASS single point positioning in an urban environment

A. Angrisano · S. Gaglione · C. Gioia

Received: 7 June 2012 / Accepted: 28 October 2012 / Published online: 15 January 2013

Abstract In signal-degraded environments such as urban canyons and mountainous area, many GNSS signals are either blocked or strongly degraded by natural and artificial obstacles. In such scenarios standalone GPS is often unable to guarantee a continuous and accurate positioning due to lack (or the poor quality) of signals. The combination of different GNSSs could be a suitable approach to fill this gap, because the multi-constellation system guarantees an improved satellite availability compared to standalone GPS, thus providing enhanced accuracy, continuity and integrity of the positioning. The present GNSSs are GPS, GLONASS, Galileo and Beidou, but the latter two are still in the development phase. In this work GPS/GLONASS systems are combined for single point positioning and their performance are assessed for different configurations. Using GPS/GLONASS multi-constellation implies the addition of an additional unknown, i.e. the intersystem time scale offset, which requires a sacrifice of one measurement. Since the intersystem offset is quasi-constant over a short period, a pseudo-measurement can be introduced to compensate the sacrifice.

The benefit after adding a pseudo-measurement has been demonstrated in a vehicular test.

Keywords Pseudorange · GPS · GLONASS · GNSS · Kalman filter · RAIM · Single point positioning

1 Introduction

GNSS (Global Navigation Satellite Systems) are worldwide, all-weather navigation systems able to provide three-dimensional position, velocity and time synchronization to UTC

A. Angrisano · S. Gaglione (✉) · C. Gioia
Department of Applied Sciences, "Parthenope" University of Naples, Napoli, Italy
e-mail: salvatore.gaglione@uniparthenope.it

A. Angrisano
e-mail: antonio.angrisano@uniparthenope.it

C. Gioia
e-mail: ciro.gioia@uniparthenope.it

(Coordinated Universal Time) scale (Hoffmann-Wellenhof et al. 1992; Kaplan and Hegarty 2006). GNSS positioning is based on satellite signal reception, hence its performance is related to signal quality, to the operational scenario and to the satellites—receiver geometry. GNSS performances are optimal in an open sky when many satellites are in view and the signals are uncorrupted; in these conditions position accuracy for single point positioning is about 10 m (Kaplan and Hegarty 2006). Satellite navigation in difficult scenarios (e.g. urban canyons, mountainous areas) is critical, because many GNSS signals are blocked or strongly degraded by various obstacles (Ackermann et al. 2012).

GPS (Global Positioning System) is a space-based radio-navigation system developed by US DoD (Department of Defense), and it is currently the most widespread GNSS. In critical environments GPS standalone is not able to provide an accurate and continuous absolute positioning; a possible approach to solving this problem is to consider the combined use of GPS with other GNSS such as Galileo, Beidou and GLONASS.

The Galileo European satellite system has presently only four satellites in orbit, i.e. the two experimental GIOVE A/B and the two Galileo satellites for the IOV (In-Orbit Validation) phase.

The Chinese satellite system Beidou is currently in the development phase.

GLONASS (Global Navigation Satellite System) is the Russian alter-ego of GPS and since 2003 it is in a modernizing phase. The GLONASS recent enhancement candidates this system as an alternative to GPS, but also as a component of multi-constellation system. In this research only GPS and GLONASS are considered.

An integrated GNSS system, composed by GPS and GLONASS, provides a significantly increased satellite availability with respect to either GPS or GLONASS alone, thereby ensuring an improvement of the positioning in harsh environments. The performance of the integrated system is improved in terms of:

- Continuity, directly related to satellite availability,
- Accuracy, enhanced by observation geometry improvement and
- Integrity, because the increased availability improves the detection process of gross errors (Angrisano et al. 2010).

The GNSS considered are quite similar to each other, but they also present several significant differences (as detailed in Sect. 2). The main difference for our purpose is related to the different time scales adopted by the systems; therefore, when GPS and GLONASS are used together, an additional unknown must be estimated, i.e. the intersystem time scale offset, thus requiring the "sacrifice" of one measurement. A possible way to fully exploit the GPS/GLONASS combination is to make use of a pseudo-measurement which takes into account the quasi-constancy characteristics of the intersystem time scale offset (Cai and Gao 2009).

One of the aims of this research is to assess the performance of different single point GNSS configurations in difficult situations, and to investigate the benefits of GLONASS inclusion to standalone GPS.

2 GNSS overview

GPS and GLONASS are similar in many aspects, such as the operational principles; they present however some meaningful differences—summarized in Table 1 and detailed in Cai 2009 and Angrisano 2010—which can be classified in three categories:

Table 1 GPS and GLONASS comparison (adapted by Cai 2009)

	Parameter	GPS	GLONASS
Constellation	Number of SV	24 (Expandable)	24
	Orbital planes	6	3
	Orbital altitude (km)	20200	19100
	Orbit inclination (deg)	55°	64.8°
	Ground track period	1 sidereal day	8 sidereal days
	Layout	Asymmetric	Symmetric
Signal	Carrier frequencies (MHz)	1575.42 1227.60	$1602 + K \times 0.5625$ $1246 + K \times 0.4375$
	Ranging code frequencies (MHz)	C/A: 1.023 L2C: 1.023 P: 10.23 M: 10.23	C/A: 0.511 P: 5.11
	Multiple access schemes	CDMA	FDMA
	Broadcast ephemerides	Keplerian	ECEF
Reference	Datum	WGS84	PZ90.02
	Time scale	GPS time	GLONASS time

- Constellation,
- Signal and
- Reference.

The aforesaid differences among GPS and GLONASS are detailed in Angrisano et al. (2012).

The main difference for our purpose is related to GPS and GLONASS time scales, which are linked with distinct UTC realizations.

In particular, GPS time is connected to UTC (USNO), maintained by the US Naval Observatory; UTC scale is occasionally adjusted by one second to keep it close to the mean solar time (connected to the astronomical definition of time). GPS time scale is indeed continuous, so it differs from UTC (USNO) for an integer number of seconds (called leap seconds). An additional difference between GPS time and UTC (USNO) must be considered because the time scales are maintained by different master clocks; this offset typically is less than 100 ns and is broadcast to the users within the GPS navigation message.

GLONASS time scale is connected to UTC (RU), maintained by Russia. GLONASS time is adjusted by leap seconds, according to the UTC adjustments, so they do not differ for an integer number of seconds, but only for a difference less than 1 millisecond, broadcast in the GLONASS navigation message.

The transformation between GPS and GLONASS times is expressed by the following formula (ICD-GLONASS 2008):

$$t_{\mathrm{GPS}} = t_{\mathrm{GLO}} + \tau_r + \tau_u + \tau_g \tag{1}$$

where $\tau_r = t_{\mathrm{UTC(RU)}} - t_{\mathrm{GLO}}$ is broadcast in the GLONASS navigation message, $\tau_u = t_{\mathrm{UTC(USNO)}} - t_{\mathrm{UTC(RU)}}$ must be estimated and $\tau_g = t_{\mathrm{GPS}} - t_{\mathrm{UTC(USNO)}}$ is broadcast in the GPS navigation message.

In order to perform the transformation (1), the difference between UTC (USNO) and UTC (RU) should be known, but this information is not provided in real-time. This problem is usually solved by including the difference between the system time scales as an unknown when GPS and GLONASS measurements are used together.

The GPS-GLONASS time offset is broadcast as a non-immediate parameter in the GLONASS almanac (ICD-GLONASS 2008), but it does not take into account the inter-system hardware delay bias which is dependent on a specific receiver (Cai and Gao 2009).

3 Estimation techniques

Estimation is the process of obtaining a set of unknowns (state vector or simply state) from a uncertain measurements set, according to a definite optimization criterion (Brown and Hwang 1997; Bar-Shalom et al. 2001). The functional relationship between measurements and state is referred to as "measurement model", whose discrete and linear version is shown below:

$$\underline{z}_k = H_k \cdot \underline{x}_k + \underline{\eta}_k \tag{2}$$

with $\underline{z}_k$ measurement vector, H_k design matrix, $\underline{x}_k$ state vector, $\underline{\eta}_k$ measurement noise vector and the subscript k representing the epoch.

The measurement model can be solved if the number of (independent) equations is at least equal to the number of unknowns. Additional equations, representing the system state dynamics, can be included in addition to the measurement model, allowing the estimation even in the case of lack of measurements. These additional equations are referred to as "process model", whose discrete and linear version is shown below:

$$\underline{x}_{k+1} = \Phi_{k+1,k} \cdot \underline{x}_k + \underline{w}_k \tag{3}$$

where $\Phi_{k+1,k}$ is the transition matrix and $\underline{w}_k$ is the process noise vector, which takes into account the model uncertainty.

The inclusion of the process model could provide a better state estimation, if the model properly represents the state behaviour. The estimation methods adopted in this research are the Least Squares technique, which only uses the measurement model, and the Kalman filter, which also uses the process model.

The LS method is the most common estimation procedure in geomatics applications and its optimization criterion is based on minimizing the sum of the square residuals, defined as:

$$\underline{r}_k = \underline{z}_k - H_k \cdot \underline{\hat{x}}_k \tag{4}$$

Different weights can be associated to each measurement in accordance with its accuracy, by weighing the accurate measurements more and the noisy ones less (Mikhail 1976; Brogan 1981).

The Kalman Filter estimation is a technique commonly used in navigation: its measurement model is formally identical to the LS one, with the additional assumption of zero-mean white noise, with Gaussian distribution for the measurement noise. The KF is a recursive algorithm using a series of prediction and update steps to obtain an optimal state vector estimate in a minimum variance sense (Kalman 1960; Brown and Hwang 1997).

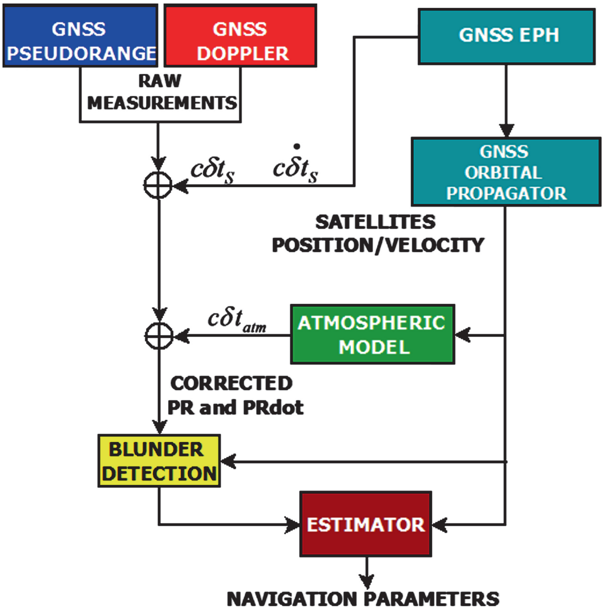

Fig. 1 PVT algorithm scheme

4 Implementation

4.1 PVT algorithm

In this research PVT (Position-Velocity-Time) algorithms (detailed in Fig. 1) are developed in Matlab environment to process GNSS data in a single point mode; the software belongs to a tool implemented at the PArthenope Navigation Group (PANG) (website http://pang.uniparthenope.it).

The main inputs are the GNSS raw measurements, i.e. pseudorange and Doppler, and the GNSS ephemerides.

The ephemerides are used to compute satellite position and velocity; different orbital propagators are implemented for the various GNSSs considered, since the ephemerides are differently parameterized. The GPS orbital propagator is extensively treated in IS-GPS-200 (2004) and Remondi (2004), while for GLONASS the main reference is ICD-GLONASS (2008).

Measurements are corrected for satellite clock offset and atmospheric errors, specifically Klobuchar and Hopfield models are adopted to reduce ionosphere and troposphere delays respectively.

A quality check is performed epoch by epoch on the corrected measurements to detect and reject gross errors; the strategy adopted is the "observation subset testing" (Kuusniemi 2005), using the global test as a decision parameter. The quality control is performed by testing the residuals in the LS case and the innovation vector in KF configurations; measurement errors are assumed to be Gaussian with zero-mean and uncorrelated. The decision variable is defined as the sum of squares of residuals (or innovation vector for KF), weighted by the measurement covariance matrix R:

$$D = \underline{r}^T \cdot R \cdot \underline{r} \tag{5}$$

and it is assumed to follow a χ^2 distribution with $(m-n)$ degrees of freedom or "redundancy", defined as the difference between the number of measurements and states.

The threshold T is usually related to the probability of false alarm P_{FA} and redundancy as shown below:

$$T = \chi^2_{1-P_{\mathrm{FA}},(m-n)} \tag{6}$$

T is the abscissa related to a probability value $(1-P_{\mathrm{FA}})$ of a chi-square distribution of $(m-n)$ order.

A common procedure consists of fixing P_{FA} according to the application requirements and letting the threshold vary with the redundancy; a typical value for the probability of false alarm is 0.1 % (Petovello 2003).

The above described procedure (global test) is applied to the whole set of measurements: if it passes the test, measurements are considered self-consistent and no rejection is carried out, otherwise the procedure is applied to all possible subsets including measurements from $(m-1)$ to $(n+1)$ in order to identify a subset passing the global test (Kuusniemi 2005).

The aforesaid blunder detection technique is applied separately to pseudorange and Doppler observations. After the blunder rejection, measurements are processed with LS and KF methods.

The PR and Doppler measurement equations are:

$$\begin{aligned} \rho &= d + c\delta t_u + \varepsilon_\rho \\ \dot{\rho} &= \dot{d} + c\dot{\delta} t_u + \varepsilon_{\dot{\rho}} \end{aligned} \tag{7}$$

where ρ and $\dot{\rho}$ are respectively the PR and Doppler measurements, d and $\dot{d}$ are the geometric distance receiver—satellite and its derivative, $c\delta t_u$ and $c\dot{\delta} t_u$ are the receiver clock offset and drift, ε_ρ and $\varepsilon_{\dot{\rho}}$ contain the residual errors.

The measurement model consists of equations as (7), linearized for the unknowns, and assumes the following expression:

$$\underline{\Delta\rho} = H \cdot \underline{\Delta x} + \underline{\varepsilon} \tag{8}$$

where $\underline{\Delta\rho}$ is the difference between actual and predicted measurements, $\underline{\varepsilon}$ is the residual error vector, $\underline{\Delta x}$ is the state vector, detailed below

$$\underline{\Delta x} = \left[\underline{\Delta P} \quad \underline{\Delta V} \quad \Delta\left(c\delta t_u^{\mathrm{GPS}}\right) \quad \Delta\left(c\dot{\delta} t_u^{\mathrm{GPS}}\right) \quad \Delta(c\delta t_{\mathrm{sys}})\right]^T \tag{9}$$

The state vector contains the receiver position, velocity and clock errors used to correct the previous navigation parameter estimate; $c\delta t_{\mathrm{sys}}$ is the difference between GPS and GLONASS time scales.

For the KF method a constant velocity model is adopted for the process, with velocity errors being modelled as a random walk process and $c\delta t_{\mathrm{sys}}$ as a random constant process to take into account its quasi-constancy (Cai and Gao 2009).

Developed PVT algorithms operate in a closed-loop mode, i.e. for every epoch the state vector is estimated and is used to correct the nominal state, then the state vector is reset to a null vector (Brown and Hwang 1997; Godha 2006). This strategy is preferred to an open-loop mode, because the errors in the estimation of navigation parameters are small enough to stay within the assumptions of the linearization process.

Fig. 2 Test trajectory

4.2 Aiding on inter-system time scale

If GPS and GLONASS measurements are used together, the difference between the systems time scales must be estimated, thus limiting a full use of multi-constellation, since one equation has to be "sacrificed" to estimate the additional unknown.

The offset between GPS and GLONASS time scales can be considered constant in a brief interval (Cai and Gao 2009), hence a pseudo-measurement, observing directly $c\delta t_{sys}$, can be introduced as follows:

$$(c\delta t_{sys\text{-}aid} - c\delta t_{sys0}) = \lfloor (0)_{1x(n-1)} \quad 1 \rfloor \cdot \underline{\Delta x} \tag{10}$$

where $c\delta t_{sys\text{-}aid}$ is an "old" estimation of the parameter, computed with low value of corresponding state variance/covariance matrix, $c\delta t_{sys0}$ is the previous state element and n is the number of states.

Equation (10) can be included in the measurement model (8), allowing a GPS/GLONASS solution in LS case with 4 mixed visible satellites; this aiding is also used in case of sufficient observables ($\geq$5 mixed satellites) to enhance measurement model redundancy.

5 Test

5.1 Description

The data is collected in a vehicular test carried out on 22nd July 2010 in the afternoon in downtown Calgary (Canada), a typical example of an urban canyon; many GNSS signals are blocked by skyscrapers or are strongly degraded by multipath effects. The test begins in a small parking lot with a static interval in good visibility conditions (9 GPS and 5 GLONASS satellites available) and continues into the central downtown where the number of visible satellites decreases significantly, thus bringing many partial and total GNSS outages during the trajectory (Fig. 3). The test ends outside downtown with good visibility conditions. Total test duration is about 30 minutes with a distance travelled of about 10 km. The vehicle speed varies from 0 to 50 km/h with frequent stops due to traffic lights. The trajectory followed by the car is shown in Fig. 2.

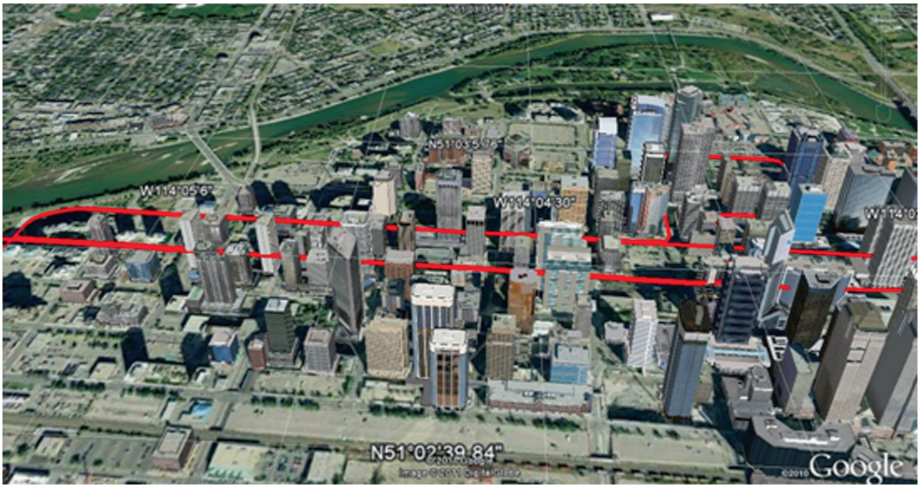

Fig. 3 Urban segment

Fig. 4 Equipment

5.2 Equipment

The receiver used is a NovAtel ProPak-V3 belonging to the OEMV family, a high-performance device able to provide L1 and L2 GPS + GLONASS positioning; the connected antenna is a high performance NovAtel 702 antenna mounted on the car roof as shown in Fig. 4.

5.3 Reference

A reference solution is generated using the NovAtel SPAN (Synchronous Position, Attitude and Navigation) system, consisting of a Honeywell HG1700, a tactical grade IMU (Inertial Measurement Unit), and an OEM4 GPS receiver. The NovAtel ProPak-V3 and OEM4 receiver are connected to the same antenna through a signal splitter. The reference solution is computed in post-mission, by processing inertial and GPS data with NovAtel Inertial Explorer software, and by using a tightly coupled strategy and a double difference technique; the GPS base station for differential processing is located 6–7 km away from the test location on the roof top of a building. The reference solution accuracy in these conditions (as estimated by the NovAtel software) is decimetric for position and cm/s for velocity.

Table 2 Position accuracy

Configurations	RMS (m)			Max (m)		
	Horizontal	Up	3D	Horizontal	Up	3D
GPS LS	11.4	20.6	23.5	196.3	210.9	278.2
GG LS	9.4	15.1	17.8	97.0	204.7	223.5
GPS KF	10.2	19.0	21.6	51.5	179.8	184.4
GG KF	9.4	7.5	12.0	54.8	41.1	61.8

6 Results and analysis

In this research 6 GNSS configurations are considered and analyzed, differing for satellite system and estimation method, specifically:

- GPS only with LS (GPS LS),
- GPS/GLONASS with LS (GG LS),
- GPS only with KF (GPS KF),
- GPS/GLONASS with KF (GG KF),
- GPS/GLONASS with LS and aiding on intersystem bias (GG LS Aiding),
- GPS/GLONASS with KF and aiding on intersystem bias (GG KF Aiding).

PR and Doppler observations are processed in single point positioning. The comparison is carried out in terms of solution availability (i.e. the percentage of time when the solution is available) and position/velocity accuracy; for a fair comparison, the accuracy analysis is only performed when the solution is obtainable for all configurations (i.e. if GPS LS fix is available).

KF solutions are continuous, hence solution availability is 100 %; GPS LS solution displays several partial and total outages (clearly visible in Fig. 5 on the top) and the fix is only possible during 61 % of the mission. The inclusion of GLONASS provides a 4 % improvement in availability (up to 65 %) and a reduction of GNSS outages (circled areas in Fig. 5).

The accuracy analysis is carried out in terms of RMS (Root Mean Square) and maximum errors on position and velocity; the relative behavior is shown in Fig. 6 and Fig. 7.

Performance analysis results are summarized in Tables 2 and 3.

The GPS/GLONASS configurations demonstrate an improved performance with respect to GPS only (line 1 versus line 2 and line 3 versus line 4 in Table 3) in both horizontal and vertical components, in terms of RMS and maximum error.

RMS horizontal errors are similar for homologous LS and KF configurations, but KF limits maximum horizontal errors. Moreover KF vertical errors are strongly limited too, since the process model is consistent with slow altitude variations in typical vehicular navigation.

From Table 3 it can be noted that velocity solutions are very similar, with only slight advantages for GPS/GLONASS over GPS only and KF over LS.

The multi-constellation approach provides improvements, in terms of solution availability and accuracy, but it introduces an additional unknown, hence one observation must be used to estimate it. The time scale offset between GPS and GLONASS time can be considered constant in a short interval, hence a pseudo-observation is used to observe the unknown directly. The pseudo-observation is based on the “old” estimate of $c\delta t_{\mathrm{sys}}$ in good accuracy condition, i.e. with a low value of the corresponding element of the solution variance/covariance matrix.

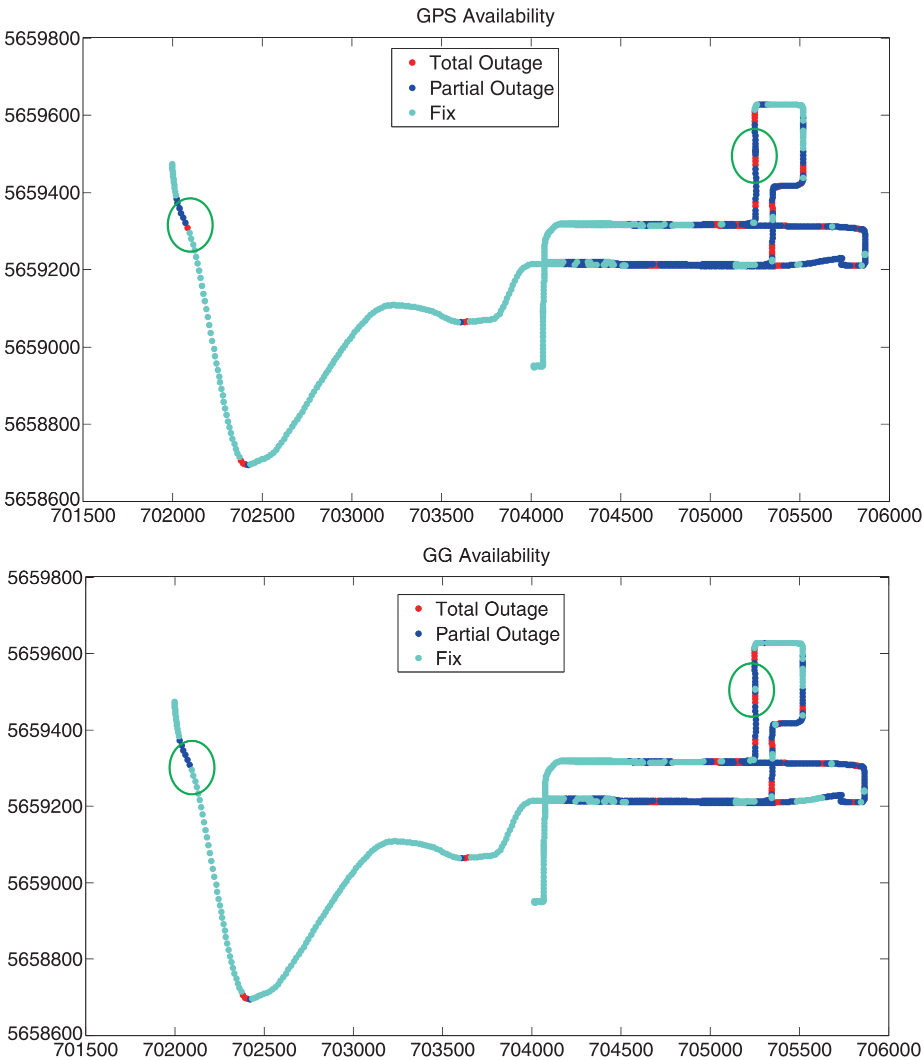

Fig. 5 LS solution availability on the trajectory

The configuration with the GG LS Aiding is compared against a standard GG LS solution, thus showing an availability improvement of 3 %, owing to the solutions performed in case of 4 mixed satellites (as shown in Table 4).

The aiding is always used (not only for the case of 4 mixed GPS/GLONASS) as an additional measurement to increase the redundancy, and it shows an improved performance with respect to the GG LS case, in both horizontal and vertical components, in terms of RMS and maximum error.

The aiding inclusion on $c\delta t_{sys}$ does not produce benefits on GG KF configuration, because the quasi-constancy of the inter-system time scale bias is already included in process model.

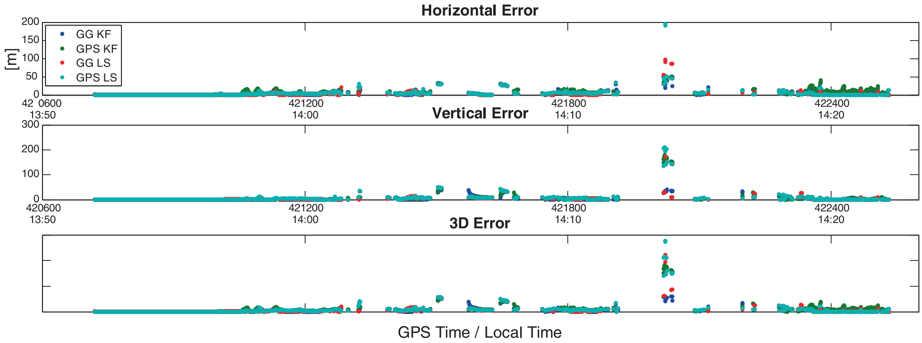

Fig. 6 Position accuracy analysis

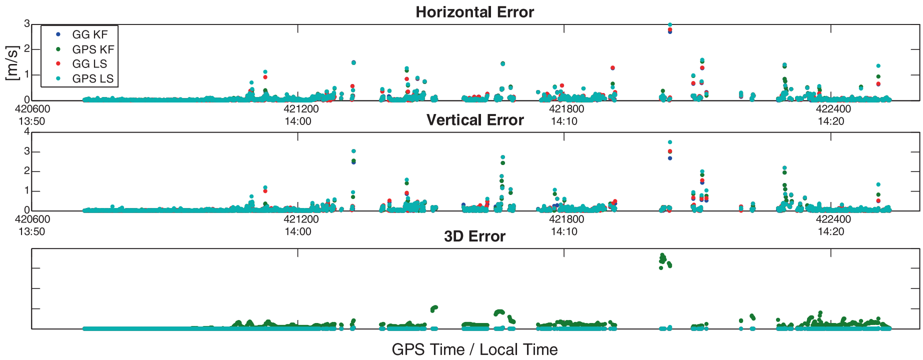

Fig. 7 Velocity accuracy analysis

Table 3 Velocity accuracy

Configurations	RMS (m/s)			Max (m/s)		
	Horizontal	Up	3D	Horizontal	Up	3D
GPS LS	0.188	0.254	0.316	2.982	3.491	4.591
GG LS	0.170	0.224	0.281	2.803	3.045	4.138
GPS KF	0.180	0.225	0.288	2.812	3.028	4.133
GG KF	0.168	0.202	0.263	2.695	2.674	3.796

7 Conclusions

Based on the research results presented in this paper, GPS/GLONASS configurations show evident improvements with respect to stand-alone GPS in terms of solution availability and accuracy, the parameters which are usually considered to be critical in urban scenarios. Least squares and Kalman Filter estimators are used to process GNSS data in single point positioning and for both methods GLONASS inclusion yields evident benefits.

The multi-constellation systems adds an additional unknown to the estimation procedure, i.e. the offset between their time scales; in order to avoid the “sacrifice” of one observation, a pseudo-measurement is introduced by observing this offset directly and by taking into

Table 4 Position accuracy and solution availability with aiding

Configurations	RMS (m)			Max (m)			Solution availability
	Horizontal	Up	3D	Horizontal	Up	3D	
GG LS	9.4	15.1	17.8	97.0	204.7	223.5	0.65
GG LS aiding	8.0	13.4	15.6	64.1	204.7	210.9	0.68

account its stability for short periods. With the aiding on the inter-system timescale bias, the required minimum satellite number for a LS solution estimate is reduced to four, rather than the five required by the standard model.

GG LS aided solution demonstrates improved availability and accuracy, while no benefits are found in GG KF case (offset quasi-constancy is already included in the process model).

LS and KF provide similar performance in terms of RMS, but KF solutions demonstrate a better performance in terms of maximum errors and for the vertical solution; this can be explained considering that the simple process model adopted, well represents the slowly varying altitude behaviour, but it is not fully consistent with the real vehicle motion and so it is only able to limit large errors in the horizontal solution.

8 Future work

The results obtained in this work demonstrate the benefit of the GLONASS inclusion; the next step will be a performance assessment of a multi-constellation system including Galileo.

Additional pseudo-measurement will be introduced in the measurement model; moving from the encouraging results of this study the Authors will investigate the performance of the aiding on the altitude at first, and will then consider the combined use of altitude and $c\delta t_{\mathrm{sys}}$ pseudo-measurements.

The development of an adaptive KF for vehicular navigation will be also included in next studies.

Acknowledgements The authors would like to thank the PLAN group (Position, Location And Navigation Group) of University of Calgary (Canada) for their valuable contribution and support and for providing the test equipment.

References

Ackermann S, Angrisano A, Del Pizzo S, Gaglione S, Gioia C, Troisi S (2012, in press) Digital surface models for GNSS mission planning in critical environment. South-East Eur J Earth Obs Geomat 1(2)

Angrisano A, Petovello MG, Pugliano G (2010) GNSS/INS integration in vehicular urban navigation. In: Proceedings of GNSS10, Portland, OR, 21–24 September. The Institute of Navigation, Portland, pp 1505–1512

Angrisano A (2010) GNSS/INS integration methods. Published thesis (PhD), "Parthenope" University of Naples

Angrisano A, Gaglione S, Gioia C (2012) RAIM algorithms for aided GNSS in urban scenario. In: Proceedings of ubiquitous positioning indoor navigation and location based service, Helsinki, 3–4 October 2012

Bar-Shalom Y, Li X, Kirubarajan T (2001) Estimation with applications to tracking and navigation. Wiley, New York

Brogan WL (1981) Improvements and extensions of GDOP concept for selecting navigation measurements

Brown RG, Hwang PYC (1997) Introduction to random signals and applied Kalman filtering. Wiley, New York

Cai C (2009) Precise point positioning using dual-frequency GPS and GLONASS measurements. Published thesis (MSc), University of Calgary, Canada

Cai C, Gao Y (2009) A combined GPS/GLONASS navigation algorithm for use with limited satellite visibility. J Navig 62:671–685

Godha S (2006) Performance evaluation of low cost MEMS-based IMU integrated with GPS for land vehicle navigation application. Published thesis (MSc), University of Calgary, Canada

Hoffmann-Wellenhof B, Lichtenegger H, Collins J (1992) Global positioning system: theory and practice. Springer, Wien

ICD-GLONASS (2008) Global navigation satellite system GLONASS interface control document. Version 5.1, Moscow

IS-GPS-200 (2004) Navstar GPS space segment/navigation user interfaces, revision D. ARINC Research Corporation, El Segundo, CA

Kalman RE (1960) A new approach to linear filtering and prediction problems. Trans ASME J Basic Eng, 35–45

Kaplan ED, Hegarty J (2006) Understanding GPS: principles and applications, 2nd edn. Artech House, London

Kuusniemi H (2005) User-level reliability and quality monitoring in satellite-based personal navigation. Published thesis (PhD). Tampere University of Technology, Finland

Mikhail EM (1976) Observations and least squares. IEP, New York

Petovello M (2003) Real-time integration of a tactical-grade IMU and GPS for high-accuracy positioning and navigation. Published thesis (PhD). University of Calgary, Canada

Remondi BW (2004) Computing satellite velocity using the Broadcast Ephemeris. GPS Solut 8(3):181–183